© 2016. Published by The Company of Biologists Ltd | Journal of Experimental Biology (2016) 219, 311-318 doi:10.1242/jeb.131441

RESEARCH ARTICLE

European shags optimize their flight behavior according to wind conditions

Yukihisa Kogure[1], Katsufumi Sato[1,*], Yutaka Watanuki[2], Sarah Wanless[3] and Francis Daunt[3]

ABSTRACT

Aerodynamics results in two characteristic speeds of flying birds: the minimum power speed and the maximum range speed. The minimum power speed requires the lowest rate of energy expenditure per unit time to stay airborne and the maximum range speed maximizes air distance traveled per unit of energy consumed. Therefore, if birds aim to minimize the cost of transport under a range of wind conditions, they are predicted to fly at the maximum range speed. Furthermore, take-off is predicted to be strongly affected by wind speed and direction. To investigate the effect of wind conditions on take-off and cruising flight behavior, we equipped 14 European shags *Phalacrocorax aristotelis* with a back-mounted GPS logger to measure position and hence ground speed, and a neck-mounted accelerometer to record wing beat frequency and strength. Local wind conditions were recorded during the deployment period. Shags always took off into the wind regardless of their intended destination and take-off duration was correlated negatively with wind speed. We combined ground speed and direction during the cruising phase with wind speed and direction to estimate air speed and direction. Whilst ground speed was highly variable, air speed was comparatively stable, although it increased significantly during strong head winds, because of stronger wing beats. The increased air speeds in head winds suggest that birds fly at the maximum range speed, not at the minimum power speed. Our study demonstrates that European shags actively adjust their flight behavior to utilize wind power to minimize the costs of take-off and cruising flight.

KEY WORDS: GPS, Accelerometer, Maximum range speed, Minimum power speed

INTRODUCTION

Flight is energetically expensive, so its regulation under variable environmental conditions is critical for flying birds to optimize energy expenditure. The cost of transport is the key to understanding bird flight, and is defined as the energy cost per air distance traveled and combines basal and activity-specific metabolic rates (Schmidt-Nielsen, 1972). Models of bird flight based on aerodynamics have proposed two flight speeds associated with continuous wing beats: the minimum power speed (V_{mp}), which requires the lowest rate of energy expenditure to keep flying; and the maximum range speed (V_{mr}), which is faster than V_{mp}, and is the speed at which the greatest air distance is covered per unit of fuel energy consumption, thus minimizing the cost of transport (Pennycuick, 2008). V_{mr} is expected to be the most cost-effective flight speed, in particular during migration or commuting between breeding and foraging sites.

Several studies have measured snapshots of flight speed under natural conditions using a theodolite (Pennycuick, 2008) or Doppler radar (Alerstam, 1990). Observed speeds typically lie between V_{mr} and V_{mp}, and in some cases birds appear to operate at V_{mr} during cruising flight (Pennycuick, 1987; Welham, 1992; Alerstam et al., 1993). However, obtaining a continuous record of flight speed across an entire cruising flight has proved more challenging. In recent years, miniaturization of animal-borne GPS (global positioning system) loggers has made it possible to obtain highly accurate locations of birds over prolonged periods and, therefore, variation in flight speed over the course of a cruising flight can readily be quantified (Weimerskirch et al., 2002). The flight speed recorded by a GPS track is the 'ground speed', i.e. the speed relative to the ground. To understand a bird's flight energy efficiency, however, an estimate of 'air speed' is also required, i.e. the speed relative to the air, as this determines the energy expended. When a bird is airborne, air speed and heading direction can be estimated by combining the ground vector from GPS data and the measured wind vector (Fig. 1).

Optimal flight theory predicts that the maximum range speed V_{mr} increases with head winds and decreases with tail winds, whilst the minimum power speed V_{mp} has a constant value irrespective of wind conditions (Hedenström et al., 2002). Many field studies have found negative correlations between air speed and wind speed (Pennycuick, 1987; Wakeling and Hodgson, 1992; Alerstam et al., 1993; Liechti et al., 1994; Spear and Ainley, 1997; Hedenström et al., 1999, 2002; Green and Alerstam, 2000; Rosén and Hedenström, 2001; Elliott et al., 2014). However, several recent studies have cautioned that comparing wind speed with air speed (i.e. ground speed−wind speed), which are not independent variables, can result in erroneous negative correlations (Liechti, 2006; Shamoun-Baranes et al., 2007). Following the approach recommended by Shamoun-Baranes et al. (2007), Yoda et al. (2012) used a two-dimensional generalized additive model (GAM) to analyze data from great cormorant *Phalacrocorax carbo* (N=4) and concluded that birds changed their air speed in relation to two wind components (north–south and east–west), thereby supporting the assertion that birds fly at the maximum range speed V_{mr}. However, it still remains unclear whether birds increase their air speed in head winds as predicted by the theory (Hedenström et al., 2002).

When investigating the effects of wind conditions on flight behavior, it is important to consider take-off as well as steady, level flight. Take-off is the transition from being supported by the Earth's surface to being supported entirely by aerodynamic forces, and it is accomplished by acceleration until the air speed reaches V_{mp} (Pennycuick, 2008). Power equivalent to several times the body weight is required for take-off (Alexander, 2003; Videler, 2005). If a bird takes off into the wind, it commences with an air speed equal to

[1]Atmosphere and Ocean Research Institute, The University of Tokyo, 5-1-5 Kashiwanoha, Kashiwa, Chiba 277-8564, Japan. [2]Graduate School of Fisheries Sciences, Hokkaido University, Minato-cho 3-1-1, Hakodate 041-8611, Japan. [3]Centre for Ecology & Hydrology, Bush Estate, Penicuik, Midlothian EH26 0QB, UK.

*Author for correspondence (katsu@aori.u-tokyo.ac.jp)

Received 3 September 2015; Accepted 12 November 2015

Journal of Experimental Biology (2016) 219, 311-318 doi:10.1242/jeb.131441

List of symbols and abbreviations

ATWC	adjusted tail wind component (m s^{-1})
b	wing span (m)
C_{Db}	body drag coefficient
C_{Dpro}	profile drag coefficient for the wings
g	acceleration due to gravity (m s^{-2})
k	induced power factor
m	body mass (kg)
P_b	basal metabolic rate of seabirds (W)
P_{chem}	total chemical power (W)
P_{ind}	induced power needed to support the weight (W)
P_{par}	parasite power needed to overcome the drag of the body (W)
P_{pro}	profile power needed to overcome the drag of the wings (W)
R	respiration factor
S_b	frontal body area (m^2)
S_w	wing area (m^2)
TWC	tail wind component (m s^{-1})
$\mathbf{V}_a$	air speed vector
V_a	air speed (m s^{-1})
$\mathbf{V}_g$	ground speed vector
V_g	ground speed (m s^{-1})
V_{mp}	the minimum power speed (m s^{-1})
V_{mr}	the maximum range speed (m s^{-1})
$\mathbf{V}_w$	wind vector
V_w	wind speed (m s^{-1})
η	efficiency to convert chemical power consumption to mechanical power output
γ	angle between the wind and heading direction
ρ	air density (kg m^{-3})
θ	angle between the wind and the GPS track

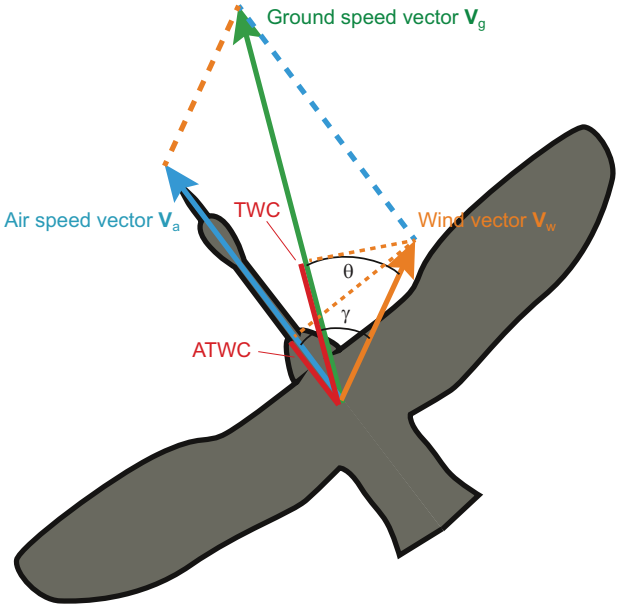

Fig. 1. Conceptual diagram of how to calculate bird air speed, tail wind component and adjusted tail wind component. Wind vector $\mathbf{V}_w$ (orange) indicates wind speed and direction from which the wind blows. Air speed vector $\mathbf{V}_a$ (blue) is composed of air speed of the bird and heading direction of the bird. Addition of the wind and air speed vectors results in the ground speed vector $\mathbf{V}_g$ (green). The ground speed vector was measured by the bird-borne GPS and the wind vector was recorded using a portable weather station in the study colony. The tail wind component TWC was calculated from wind speed and the angle θ between the wind and ground speed vectors. The adjusted tail wind component ATWC was calculated from wind speed and the angle γ between the wind and air speed vectors.

the wind speed, which greatly reduces the effort required to take off and accelerate to V_{mp} (Pennycuick, 2008).

The aim of the present study was to investigate the flight strategy of European shags *Phalacrocorax aristotelis* (Linnaeus 1762) in relation to wind conditions both at take-off and during cruising flight. We deployed back-mounted GPS and neck-mounted accelerometers on 14 adult males to measure ground vectors and flight effort (wing beat frequency and strength). By combining wind vectors (speed and direction) measured by a portable weather station at the study colony, air vectors of birds were calculated every 5 min. This enabled the tail wind component in the direction of flight and adjusted tail wind component in the heading direction (Fig. 1) to be compared with ground speed, air speed and flight effort to determine whether birds used V_{mp} or V_{mr} during their cruising flight. We also tested how wind conditions affected take-off direction and effort.

MATERIALS AND METHODS

Fieldwork and instruments

Fieldwork was conducted on the Isle of May, Scotland (56°11′N, 02°33′W) during the chick-rearing period in June 2008, 2009 and 2010. The work was conducted under research licenses from Scottish Natural Heritage and the British Trust for Ornithology. We captured 14 males at the nest using a crook attached to a bamboo pole, in the evening or early morning (6 birds in 2008, 5 birds in 2009, 3 birds in 2010; Table 1). Birds were weighed and instrumented with an accelerometer on the neck and a GPS logger on the back, using waterproof tape (Tesa™ tape, Beiersdorf AG, Hamburg, Germany). Mean handling time was 9±3 min (maximum handling time 18 min). After release, birds returned to their nests within a few minutes in all cases where the mate had not assumed nest duties. After 24 h, birds were recaptured and the loggers removed. We measured body mass again and the lighter of the two masses was assumed to reflect the body mass of the individual (kg) with an empty stomach. Body girth (m), wing span (m) and wing area (m^2) were also recorded. All devices were recovered successfully from birds and we obtained data from all individuals.

Two types of accelerometer and one type of GPS logger were used: M190L-D2GT (15 mm diameter, 53 mm length, 16 g in the

Table 1. Body mass, number of trips recorded and details on flight performance of each individual (male)

Bird ID	Body mass (kg)	No. of trips	No. of flights	Total duration of flights (min)	Max. distance from colony (km)
0804	1.91	2	5	40	7.6
0806	1.86	2	10	12	8.5
0813	1.87	2	11	23	8.3
0816	1.78	3	10	24	9.9
0821	1.78	2	15	48	10.5
0823	2.04	4	10	23	4.6
0901	1.84	3	14	55	11.8
0902	1.91	3	10	63	12.3
0903	1.76	3	11	50	9.4
0904	1.84	2	14	31	11.1
0905	1.77	2	8	36	11.3
1011	1.91	4	22	94	7.4
1021	1.80	3	31	59	10.7
1025	1.79	3	20	37	10.5

Journal of Experimental Biology

Journal of Experimental Biology (2016) 219, 311-318 doi:10.1242/jeb.131441

air; Little Leonardo Ltd, Tokyo, Japan) that recorded two-axis acceleration (64 Hz), depth (1 Hz) and temperature (1 Hz) in 2008 and 2009; ORI400-D3GT (12 mm diameter, 45 mm length, 9 g in the air; Little Leonardo Ltd) that recorded three-axis acceleration (50 Hz), depth (1 Hz) and temperature (1 Hz) in 2010; GPL20 (49 mm width and length, 21 mm depth, 61 g in the air; Little Leonardo Ltd) that recorded longitude and latitude (1 Hz). The combined mass of the GPS and accelerometer was 4.2±0.3% (N=14) of the birds' body masses.

During the study, average wind speed and direction (wind vector) in a 16-wind compass rose was recorded every 5 min in 2008 and 2009 and every minute in 2010 using a portable weather station (WS 3502, La Crosse Technology Ltd, USA) positioned close to the highest point on the island (altitude ca. 65 m above sea level). Because all foraging trips occurred within 12 km of the colony (Table 1), supporting previous findings in this population (Bogdanova et al., 2014), we considered that our wind data were representative of the wind conditions experienced by all study individuals whilst on foraging trips. To make the wind data comparable across years, the data set from 2010 was sub-sampled at 5 min intervals.

Data analysis

Behavioral analyses were carried out in Igor Pro (WaveMetrics, Inc., Lake Oswego, OR, USA) using the package Ethographer (Sakamoto et al., 2009). We used longitudinal acceleration to analyze wing beats. Acceleration data were recorded in $\boldsymbol{g}$ with the D3GT. For the latter, acceleration in $\boldsymbol{g}$ was converted into m s^{-2} using the conversion of 1 $\boldsymbol{g}$ to 9.8 m s^{-2}. To calibrate the values recorded by the D2GT loggers, values were recorded by each logger set at angles of 90 and −90 deg to the horizontal. These data were divided into static acceleration (i.e. gravity) and specific acceleration caused by the bird's movements, using a low-pass filter (<1.5 Hz) (Sato et al., 2003). From this high-frequency component of acceleration, we extracted two important measures of flight effort. Wing beat frequency was calculated every second using wavelet transformation and wing beat strength was calculated as the average of absolute amplitude of each waveform every second.

Longitude and latitude data were converted into UTM coordinates, and then horizontal ground speed and flight direction (ground vector) were calculated every second for sequential location points. During foraging trips, ground speed showed a tri-modal frequency distribution: the lowest peak (at speeds of 0 to 0.5 m s^{-1}) represented resting behavior on the water surface or on land, and the two higher peaks represented dominant speeds during flight.

A flight was defined as any continuous sequence of high-speed (>1 m s^{-1}) movement lasting a minimum of 60 s. This relatively low speed threshold was chosen so that flight included both take-off and cruising flight. In total, 191 flights were identified for analysis. Each flight was partitioned into the take-off and cruising flight phases based on wing beat frequency. As described in a previous paper (Sato et al., 2008), European shags made continuous wing beats throughout their flights, but wing beat frequency was higher at the start and then declined to a constant lower value during the cruising phase. To identify the dominant wing beat frequency of each flight, the power spectral density (PSD) was calculated, and we then defined the take-off phase as the initial part of each flight when the wing beat frequency was 3% higher than the dominant frequency of each flight. Because proximity to land can affect micro-scale wind conditions, we excluded all take-offs that occurred within 200 m of the shore. This reduced our sample size from 191 to 147 flights.

Table 2. Results of AIC values from a generalized linear mixed effect model (family=Gaussian)

Response variables	Explanatory variables	AIC
Take-off duration	Null	843.9
	Wind speed	**829.5**
Wing beat frequency during take-off	**Null**	**148.6**
	Wind speed	149.6
Wing beat strength during take-off	Null	746.2
	Wind speed	**741.4**
Ground speed during cruising flight	Null	187,415
	TWC	**151,517**
Air speed during cruising flight	Null	151,547
	ATWC	**150,344**
Wing beat frequency during cruising flight	**Null**	**−32,156**
	ATWC	−32,150
Wing beat strength during cruising flight	Null	142,531
	ATWC	**141,222**

Individual was fitted as a random effect. The best models are shown in bold. TWC, tail wind component; ATWC, adjusted tail wind component.

Calculation of air speed and tail wind components

Every second, the air speed vector $\mathbf{V}_a$ was calculated by subtracting the wind vector $\mathbf{V}_w$ from the ground speed vector $\mathbf{V}_g$ (Fig. 1):

$$\mathbf{V}_a = \mathbf{V}_g - \mathbf{V}_w. \quad (1)$$

Also, as indices of the wind effect on flight speed, we calculated the tail wind component (TWC) and the adjusted tail wind component (ATWC) as:

$$\mathrm{TWC} = |V_w| \cos\theta, \quad (2)$$

$$\mathrm{ATWC} = |V_w| \cos\gamma, \quad (3)$$

where V_w is wind speed (m s^{-1}), θ is the angle between the wind and the GPS track and γ is the angle between the wind and heading directions (Fig. 1). TWC was used to evaluate how ground speed in the direction of flight was influenced by the wind, whereas ATWC was used to evaluate how air speed in the heading direction was affected by the wind.

Statistics

To test the relationship between directional parameters, a V-test (a modification of the Rayleigh test) was used (Zar, 2010). Generalized linear mixed models (GLMMs) in R (R Development Core Team, 2009) were used to evaluate effects of wind (m s^{-1}) on duration, wing beat frequency and strength during take-off, and the ground speed, air speed and wing beat efforts during cruising flight. Individual was treated as a random effect and models including the above explanatory parameters were compared with null models on the basis of the Akaike information criterion (AIC) (Table 2). Additionally, a two-dimensional generalized additive model (GAM) was used to analyze the relationship between air speed and wind (Shamoun-Baranes et al., 2007). Following a previous study (Yoda et al., 2012), we divided the wind variable into two components (north–south and east–west). The two variables were implemented in a GAM by first transforming them via a LOESS smoother with a maximum span of 80% and 2 degrees of freedom, following previous studies (Shamoun-Baranes et al., 2007; Yoda et al., 2012). To fit the GAM, we used the gam package in R (R Development Core Team, 2009; Hastie, 2012). Means (±s.d.) are presented.

Journal of Experimental Biology (2016) 219, 311-318 doi:10.1242/jeb.131441

Flight models

To estimate the relationship between flight air speed (m s^{-1}) and total power required to fly (W), a power curve was calculated using two models (Norberg, 1990; Pennycuick, 2008). The models add three mechanical components of power, the induced power P_{ind} (needed to support the weight), the parasite power P_{par} (needed to overcome the drag of the body) and the profile power P_{pro} (needed to overcome the drag of the wings), and then estimate the total chemical power P_{chem} using the following equation:

$$P_{chem} = R[(P_{ind} + P_{par} + P_{pro})/\eta + P_b], \quad (4)$$

where R is the respiration factor (R=1.1) (Pennycuick, 2008), η is the efficiency to convert chemical power consumption to mechanical power output (η=0.23) (Pennycuick, 2008) and P_b is the basal metabolic rate of seabirds estimated from body mass m (P_b=5.43$m^{0.72}$) (Ellis and Gabrielsen, 2002). Although the concept outlined above is the same in the two models, Pennycuick's model assumes that profile power is constant at medium speeds between V_{mp} and V_{mr}, and calculates the minimum power speed V_{mp} and the maximum range speed V_{mr} using the following equations:

$$V_{mp} = \left(\frac{4km^2g^2}{3\rho^2\pi b^2 S_b C_{Db}}\right)^{1/4}, \quad (5)$$

$$V_{mr} = \left(\frac{4km^2g^2}{\rho^2\pi b^2 S_b C_{Db}}\right)^{1/4}, \quad (6)$$

where k is the induced power factor (k=1.2) (Pennycuick, 2008), $\boldsymbol{g}$ is acceleration due to gravity ($\boldsymbol{g}$=9.816 m s^{-2}) at mean sea level at the study site (latitude 56 deg) (Pennycuick, 2008), ρ is air density (ρ=1.226 kg m^{-3}) (Pennycuick, 2008), b is wing span, S_b is frontal body area and C_{Db} is body drag coefficient (C_{Db}=0.28) (Ribak et al., 2005). In contrast, Norberg's model considers that profile power is dependent on air speed, and calculates V_{mp} and V_{mr} using the following equations:

$$V_{mp} = \left\{\frac{4km^2g^2}{3\rho^2\pi b^2(S_b C_{Db} + S_w C_{Dpro})}\right\}^{1/4}, \quad (7)$$

$$V_{mr} = \left\{\frac{4km^2g^2}{\rho^2\pi b^2(S_b C_{Db} + S_w C_{Dpro})}\right\}^{1/4}, \quad (8)$$

where S_w is wing area and C_{Dpro} is the profile drag coefficient for the wings (C_{Dpro}=0.02) (Rayner, 1979). Equations for the two models differ slightly and Norberg's model estimates smaller values for V_{mp} and V_{mr} (Fig. 2A).

For this calculation, the following estimates of morphological parameters were used: total body mass m=1.90 kg (the mean recorded empty body mass of 1.82±0.06 kg plus the mass of the loggers, 0.08 kg); wingspan b=1.05±0.02 m; wing area S_w=0.162±0.04 m^2; frontal body area S_b=0.00991 m^2 (from measured body girth+frontal area of GPS logger). Wing

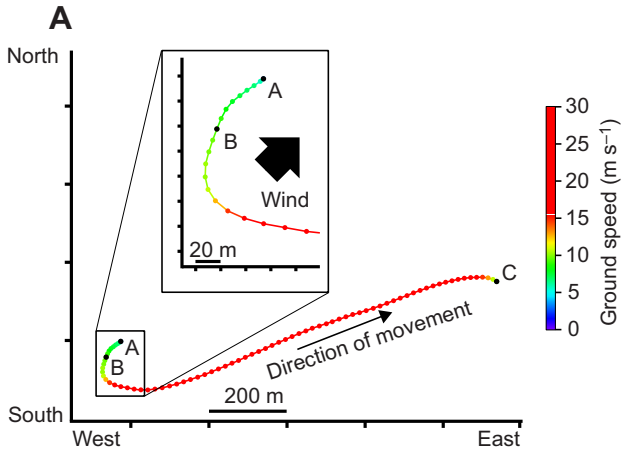

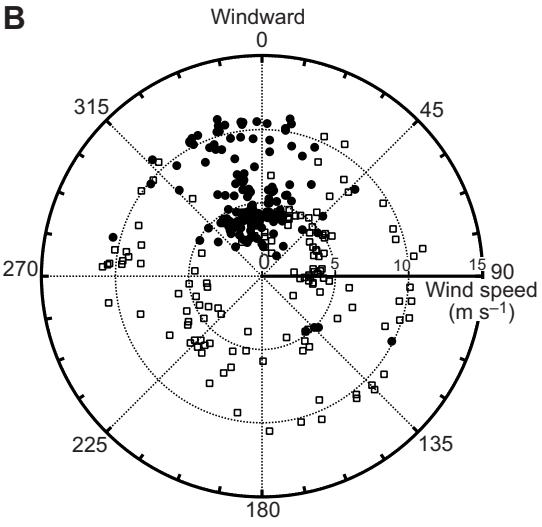

Fig. 3. Effect of wind direction on take-off direction. (A) An example GPS track of a short flight from A to C (bird ID: 1025; 11 June 2010). A–B is the take-off phase and B–C is the cruising phase. Take-off direction was defined as the direction from A to the next point. Cruising direction was defined as the direction from B to C. (B) Plot of angular differences between wind direction and take-off direction (filled circles; N=147) or cruising direction (open squares; N=147). The radial axis is the wind speed.

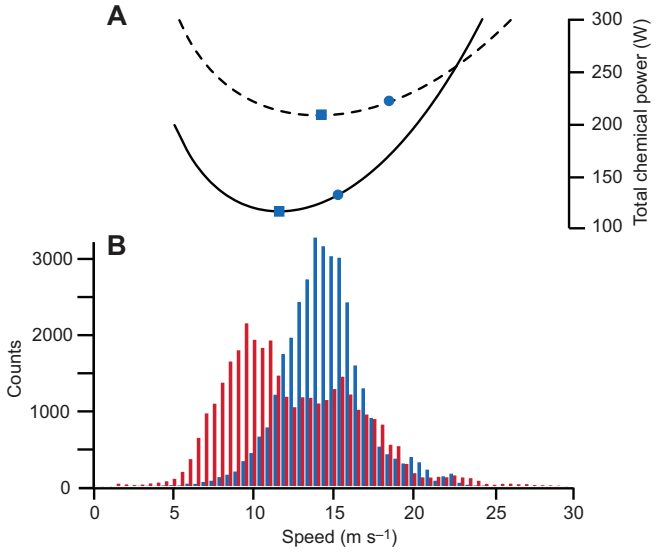

Fig. 2. Comparison of measured speed with models. (A) Total metabolic power curve of European shags based on the Pennycuick (2008) model (dotted curve) and the Norberg (1990) model (solid curve). Minimum power speed (squares; 14.0 and 11.5 m s^{-1}, respectively) and maximum range speed (circles; 18.4 and 15.2 m s^{-1}, respectively) are shown in both models. (B) Histograms of air speed (blue bars; N=33,948) and ground speed (red bars; N=33,952).

Journal of Experimental Biology

Journal of Experimental Biology (2016) 219, 311-318 doi:10.1242/jeb.131441

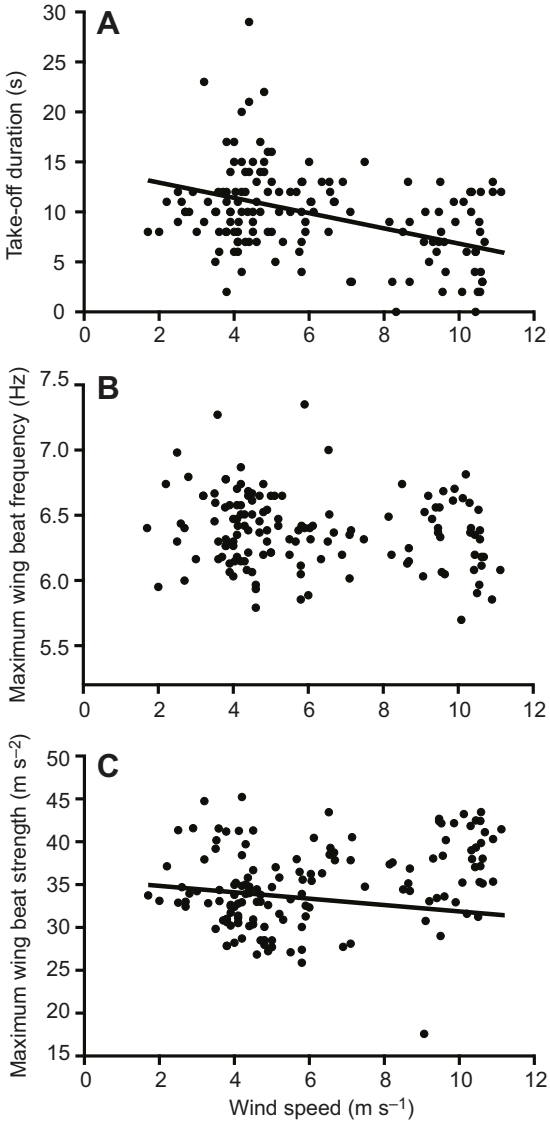

Fig. 4. Effect of wind speed on take-off. Relationship between wind speed (*N*=147) and (A) take-off duration, (B) wing beat frequency and (C) wing beat strength. The line is determined from the GLMM.

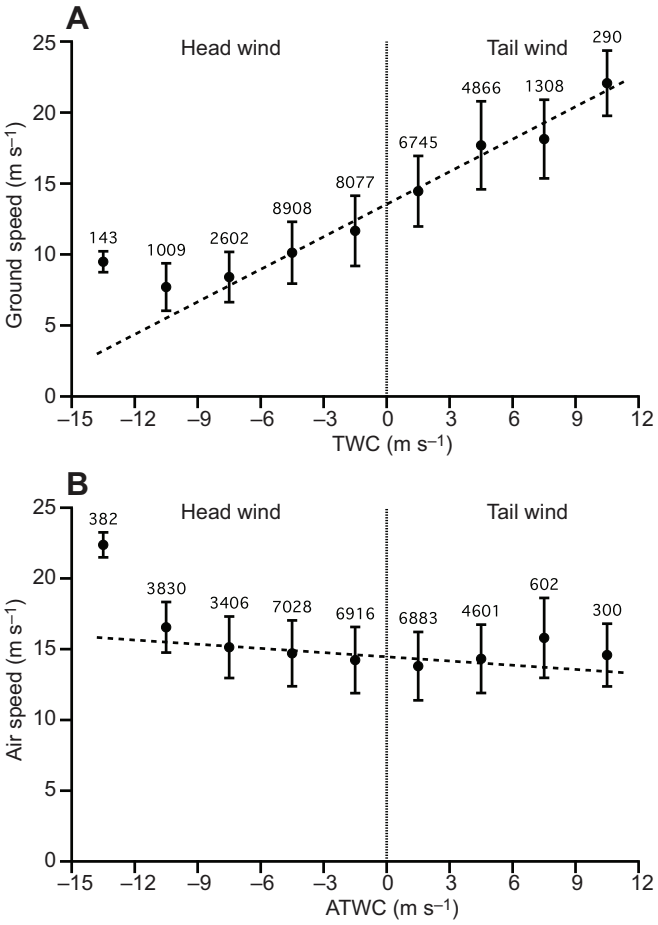

Fig. 5. Effect of wind speed on cruising flight speed. Relationship between (A) TWC and ground speed. (B) Relationship between ATWC and air speed. Lines were determined from the GLMM. Numbers above s.d. bars are sample sizes.

morphology was obtained from 5 males in 2009. Frontal body area was calculated from the mean girth of 9 individuals in 2008 and 2010 (0.334±0.013 m, *N*=9). To estimate wing morphology, we photographed the bird's wing alongside an acrylic sheet with a 50 mm grid drawn on it. Each photograph was loaded into Photoshop CS5 Extended (Adobe Systems, San Jose, CA, USA), and wingspan and wing area were calculated.

RESULTS

Take-off phase

Birds took off into the wind irrespective of the direction of their destination (Fig. 3A), with take-off directions significantly associated with wind direction (Fig. 3B; *V*-test, $P<0.0005$, *N*=147). In contrast, there was no significant relationship between cruising direction to destination and wind direction (Fig. 3B; *V*-test, $P>0.05$, *N*=147).

On average, take-off duration lasted 9.9±4.4 s (range 0–29 s, *N*=147) and take-offs were significantly shorter at higher wind speeds (Fig. 4A, Table 2). In two cases when wind speeds were greater than 8 m s^{-1}, birds became airborne without a take-off phase (Fig. 4A). Wing beat frequency during the take-off phase was not affected by wind speed but wing beat strength showed a negative relationship (Fig. 4B,C, Table 2).

Cruising phase

During the cruising phase, ground speed had a bimodal distribution, with peaks at 9.5–10.0 m s^{-1} and 15.5–16.0 m s^{-1}, while air speed had a single peak at 14.0–14.5 m s^{-1} (14.7±2.6 m s^{-1}). The mode and the mean of air speed were between the maximum range speed estimated from the Norberg model (15.2 m s^{-1}) and the minimum power speed of the Pennycuick model (14.0 m s^{-1}) (Fig. 2).

Ground speed increased significantly with the tail wind component in the direction of flight (Fig. 5A, Table 2). A generalized linear mixed model estimated V_g=13.54+0.76TWC, where V_g and TWC are ground speed and tail wind component, respectively. A two-dimensional GAM indicated that air speed was significantly related to both or one of the wind components (north–south and east–west) in all individuals ($P<0.001$). Air speed decreased significantly with the adjusted tail wind component (Fig. 5B, Table 2). A GLMM estimated V_a=14.46–0.10ATWC, where V_a and ATWC are the air speed and adjusted tail wind component, respectively. Wing beat frequency (5.50±0.20 Hz) was not related to ATWC but wing beat strength varied with ATWC (Fig. 6, Table 2).

Journal of Experimental Biology (2016) 219, 311-318 doi:10.1242/jeb.131441

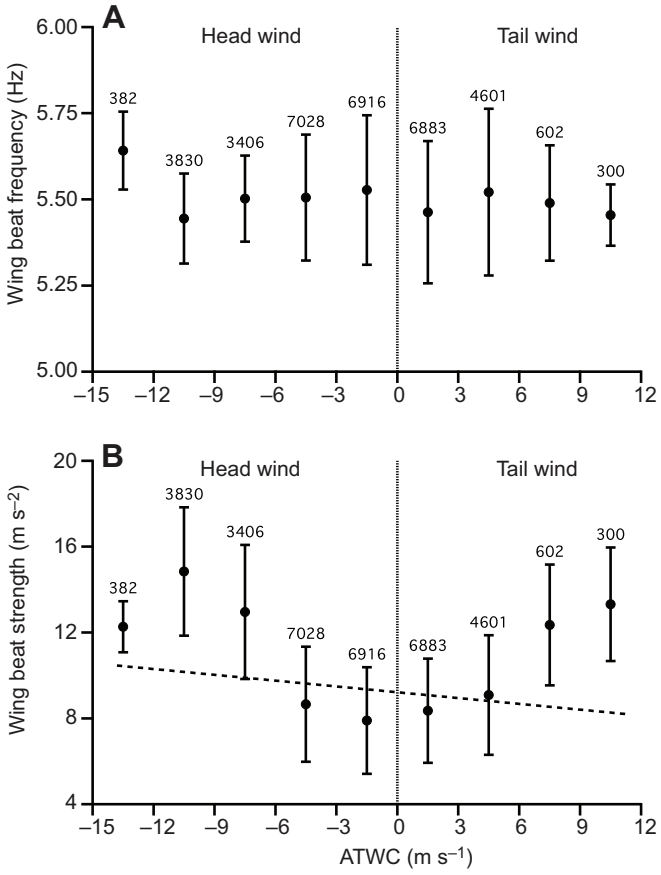

Fig. 6. Effect of wind speed on cruising flight effort. Relationship between ATWC and (A) wing beat frequency and (B) wing beat strength. The line is determined from the GLMM. Numbers above s.d. bars are sample sizes.

DISCUSSION

Strategies to minimize effort during take-off

When seabirds take off from the sea surface, they usually beat their wings at higher frequencies compared with cruising flight (Sato et al., 2008, 2009). This implies greater energy expenditure during take-off. The open nature of the sea surface, typically without any obstructions, allows birds to take off into the wind in most situations, which helps birds to generate lift with less time and effort (Pennycuick, 2008). Anecdotal field observations have long suggested that waterbirds take off into the wind, but our study appears to be the first to demonstrate this empirically. Energy expenditure during the take-off phase should increase with the duration of take-off, and the frequency and strength of wing beats. The decreased take-off duration and wing beat strength with increasing wind speed indicates that European shags reduce energy expenditure by using wind speed to gain lift.

Air speed during cruising flight

With the exception of the flightless cormorant *Phalacrocorax harrisi* (Livezey, 1992), birds in the family Phalacrocoracidae (shags and cormorants) fly by wing flapping and dive by foot stroking (Nelson, 2005). The foot-propelled method of diving has impacted on flight performance because of the additional body mass associated with the highly developed foot muscles. Watanabe et al. (2011) measured air speeds of Kerguelen shags *Phalacrocorax verrucosus* directly by propeller-based animal-borne loggers and suggested that in this deep-diving species (mean 23.5 m, maximum 108.5 m) (Cook et al., 2008; Watanabe et al., 2011), birds flew at the minimum power speed, not the maximum range speed. They speculated that this might reflect a trade-off with diving ability, resulting in relatively poor flight performance in this species. European shags have a smaller body mass and smaller wing loading (see Materials and methods) than Kerguelen shags (Watanabe et al., 2011). This means that the air speed of European shags should be slower than that of Kerguelen shags if both species fly at the minimum power speed. However, the average air speed of European shags (14.7±2.6 m s^{-1}) was not slower than that of Kerguelen shags (12.7 m s^{-1}). As shown in Fig. 2, the average air speed of European shags lies between the maximum range speed V_{mr} based on the Norberg model (15.2 m s^{-1}) and the minimum power speed V_{mp} based on the Pennycuick model (14.0 m s^{-1}). It is difficult to decide whether shags chose V_{mp} or V_{mr} because there is variation in air and wind speeds due to measurement error and uncertainties in morphological and aerodynamic parameters, which affects the calculated optimal speeds (V_{mp} and V_{mr}) and air speed (V_a). Given this uncertainty, we used the qualitative prediction derived from flight mechanical theory (Hedenström et al., 2002) and focused our interpretation on variation in air speed in relation to winds (see below).

Maximum range speed or minimum power speed

The maximum range speed (V_{mr}) is defined as the air speed (V_a) that minimizes P_{chem}/V_a, which is the energy consumed per 'air distance' traveled. As shown in Fig. 7A, this speed is the tangent from the origin of the power curve, the latter representing the relationship between total chemical power and flight air speed in calm wind conditions. If we consider the situation in a direct head wind or tail wind (i.e. where TWC matches ATWC), the maximum range speed (V_{mr}) is defined as the air speed that minimizes $P_{chem}/(V_a+TWC)=P_{chem}/V_g$ and varies with wind by drawing the tangent from the point where TWC has been reduced or added (Fig. 7A). In general, ground speed will be faster in tail wind conditions and a linear relationship between the tail wind component and ground speed is expected if a bird chooses the minimum power speed (Fig. 7B). However, if a bird chooses the maximum range speed (V_{mr}) incorporating the wind, air speed would become faster in a head wind and slower going asymmetrically towards the minimum power speed (V_{mp}) in a tail wind (Fig. 7C). In contrast, if a bird flies at the minimum power speed (V_{mp}), air speed would be constant (Fig. 7C).

Our results showed that increasing ATWC resulted in a decrease in air speed while increasing TWC caused a non-linear increase in ground speed (Fig. 5). Curves of both ground speed and air speed are similar to the predicted curves of the maximum range speed in Fig. 7B,C, in which a bird is assumed to fly at the maximum range speed (V_{mr}). Yoda et al. (2012) found that great cormorants also changed their air speed depending on the wind. These results therefore provide strong evidence that European shags (mean body mass 1.8 kg) and great cormorants (mean body mass 1.9 kg) (Yoda et al., 2012) do not fly at the minimum power speed (V_{mp}), in contrast to Kerguelen shags (mean body mass 2.2–2.5 kg) (Watanabe et al., 2011), and as such they have the capacity to adjust their air speed to minimize the cost of transport during cruising flight. In addition, our acceleration data showed that wing beat strength during flight increased during head winds (Fig. 6B). This suggests that European shags adjust flight effort to attain the maximum range speed (V_{mr}) depending on the wind conditions, such that birds increased wing beat strength in strong head winds to increase air speed.

Journal of Experimental Biology

Journal of Experimental Biology (2016) 219, 311-318 doi:10.1242/jeb.131441

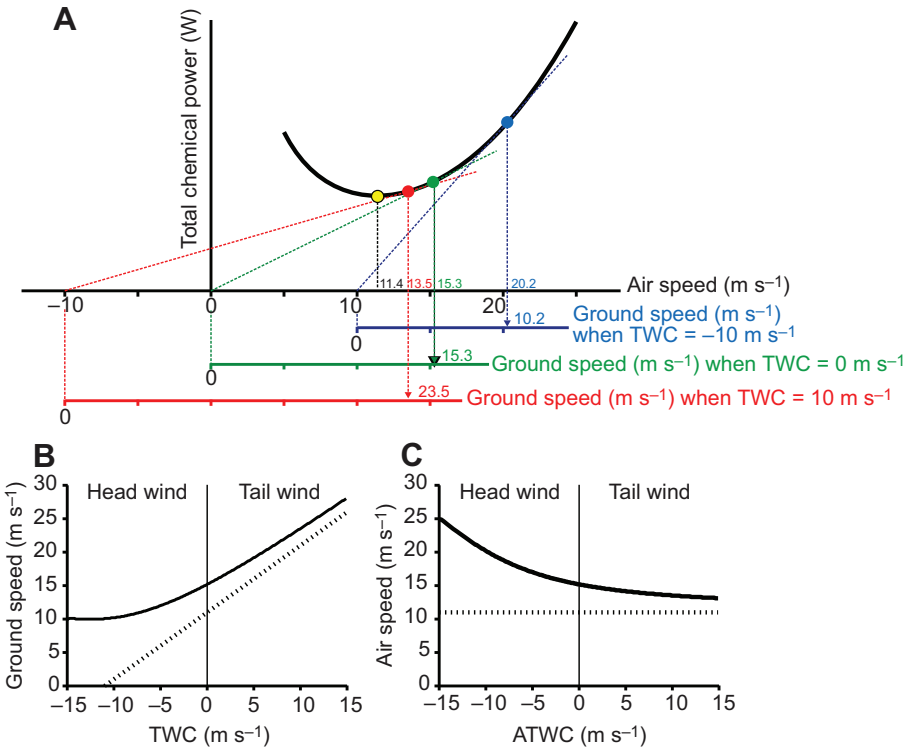

Fig. 7. V_{mr} versus V_{mp}. (A) Conceptual diagram of the Norberg (1990) model showing how maximum range speed (V_{mr}) changes in relation to TWC during a head or tail wind. The yellow dot represents minimum power speed (V_{mp}). Red, green and blue dots show maximum range speed (V_{mr}), when TWC is 10, 0 and –10 m s^{-1}, respectively. (B,C) TWC or ATWC component in relation to (B) ground speed and (C) air speed when birds fly at maximum range speed (V_{mr}; solid curve) and minimum power speed (V_{mp}; dotted line).

This finding should be taken into consideration when estimating body mass changes from the difference in wing beat frequencies during flights. Sato et al. (2008) developed a novel method to estimate temporal changes in body mass of European shags during foraging trips from changes in wing beat frequency recorded by accelerometers based on the theoretical expectation that the square root of body mass is determined by the amplitude and frequency of wing beat. Assuming that birds keep a constant air speed and wing beat amplitude, body mass change can be estimated from measured wing beat frequencies. According to the present study, these assumptions seem to be correct in calm wind conditions between −5 and 5 m s^{-1} (Fig. 5B, Fig. 6B). However, the increase in air speed in strong head wind conditions (<−12 m s^{-1}; Fig. 5B) should be considered when applying this technique to European shags and other species.

Our findings also have potential implications for shags and other volant birds engaged in flapping flight under future climatic change. Climate models are predicting that mean wind speeds will increase in many regions (McInnes et al., 2011; Young et al., 2011), which may have important consequences on foraging energetics. A recent study on European shags suggests that daily foraging time decreased with increasing wind speed (Lewis et al., 2015), which suggests that increased wave action reduces prey capture rates such that it becomes less economical to continue feeding, and hence birds return sooner to land (Daunt et al., 2006). Here, we show that flight performance is also affected by wind. However, the consequences of changing wind patterns may be complex; whilst wing beat flight may prove more energetically costly as wind speed increases, this may be offset by energy saved during take-off. These effects are likely to differ substantially among species due to factors such as local hydrographic conditions, above versus below sea surface effects and flight style (i.e. the relative reliance on flapping, gliding and soaring flight) (Ainley et al., 2015).

Acknowledgements

We thank Scottish National Heritage and the British Trust for Ornithology for permission to work on the Isle of May, Akinori Takahashi, Kentaro Sakamoto and Takashi Yamamoto for providing loggers and extensive assistance in the field, Ken Yoda for valuable advice on data analysis, and two anonymous referees for comments on an earlier version of this paper.

Competing interests

The authors declare no competing or financial interests.

Author contributions

Y.K. and K.S. analyzed the data and wrote the manuscript. All authors (Y.K., K.S., Y. W., S.W. and F.D.) attended the field study, and contributed to interpreting results and improvement of this paper.

Funding

This study was supported by Bio-logging Science, University of Tokyo, and the Natural Environment Research Council (UK).

References

Ainley, D. G., Porzig, E., Zajanc, D. and Spear, L. B. (2015). Seabird flight behavior and height in response to altered wind strength and direction. *Mar. Ornithol.* **43**, 25-36.

Alerstam, T. (1990). *Bird Migration*. Cambridge: Cambridge University Press.

Alerstam, T., Gudmundsson, G. A. and Larsson, B. (1993). Flight tracks and speeds of Antarctic and Atlantic seabirds: radar and optical measurements. *Philos. Trans. R. Soc. Lond. B Biol. Sci.* **340**, 55-67.

Alexander, R. M. (2003). *Principles of Animal Locomotion*. Princeton: Princeton University Press.

Bogdanova, M. I., Wanless, S., Harris, M. P., Lindström, J., Butler, A., Newell, M. A., Sato, K., Watanuki, Y., Parsons, M. and Daunt, F. (2014). Among-year and within-population variation in foraging distribution of European shags *Phalacrocorax aristotelis* over two decades: implications for marine spatial planning. *Biol. Conserv.* **170**, 292-299.

Cook, T. R., Lescroël, A., Trembray, Y. and Bost, C.-A. (2008). To breathe or not to breathe? Optimal breathing, aerobic dive limit and oxygen stores in deep-diving blue-eyed shags. *Anim. Behav.* **76**, 565-576.

Daunt, F., Afanasyev, V., Silk, J. R. D. and Wanless, S. (2006). Extrinsic and intrinsic determinants of winter foraging and breeding phenology in a temperate seabird. *Behav. Ecol. Sociobiol.* **59**, 381-388.

Elliott, K. H., Chivers, L. S., Bessey, L., Gaston, A. J., Hatch, S. A., Kato, A., Osborne, O., Ropert-Coudert, Y., Speakman, J. R. and Hare, J. F. (2014).

Windscapes shape seabird instantaneous energy costs but adult behavior buffers impact on offspring. *Mov. Ecol.* **2**, 17.
Ellis, H. I. and Gabrielsen, G. W. (2002). Energetics of free-ranging seabirds. In *Biology of Marine Birds* (ed. E. A. Schreiber and J. Burger), pp. 359-407. Boca Raton, FL: CRC Press.
Green, M. and Alerstam, T. (2000). Flight speeds and climb rates of Brent geese: mass-dependent differences between spring and autumn migration. *J. Avian Biol.* **31**, 215-225.
Hastie, T. (2012). "Gam: generalized additive models," R package version 1.06.2, http://cran.r-project.org/web/packages/gam/.
Hedenström, A., Rosen, M., Akesson, S. and Spina, F. (1999). Flight performance during hunting excursions in Eleonora's falcon *Falco eleonorae*. *J. Exp. Biol.* **202**, 2029-2039.
Hedenström, A., Alerstam, T., Green, M. and Gudmundsson, G. A. (2002). Adaptive variation of airspeed in relation to wind, altitude and climb rate by migrating birds in the Arctic. *Behav. Ecol. Sociobiol.* **52**, 308-317.
Lewis, S., Phillips, R. A., Burthe, S. J., Wanless, S. and Daunt, F. (2015). Contrasting responses of male and female foraging effort to year-round wind conditions. *J. Anim. Ecol.* **84**, 1490-1496.
Liechti, F. (2006). Birds: blowin' by the wind? *J. Ornithol.* **147**, 202-211.
Liechti, F., Hedenström, A. and Alerstam, T. (1994). Effects of sidewinds on optimal flight speed of birds. *J. Theor. Biol.* **170**, 219-225.
Livezey, B. C. (1992). Flightlessness in the Galápagos cormorant (*Compsohalieus [Nannopterum] harrisi*): heterochrony, giantism and specialization. *Zool. J. Linn. Soc.* **105**, 155-224.
McInnes, K. L., Erwin, T. A. and Bathols, J. M. (2011). Global climate model projected changes in 10 m wind speed and direction due to anthropogenic climate change. *Atmos. Sci. Lett.* **12**, 325-333.
Nelson, J. B. (2005). *Pelicans, Cormorants, and their Relatives*. New York: Oxford University Press.
Norberg, U. M. (1990). *Vertebrate Flight: Mechanics, Physiology, Morphology, Ecology and Evolution*. Berlin: Springer-Verlag.
Pennycuick, C. J. (1987). Flight of auks (Alcidae) and other northern seabirds compared with southern Procellariiformes: ornithodolite observations. *J. Exp. Biol.* **128**, 335-347.
Pennycuick, C. J. (2008). *Modelling the Flying Bird*. Amsterdam, Boston, Heidelberg, London, New York, Oxford, Paris, San Diego, San Francisco, Singapore, Sydney, Tokyo: Academic Press.
R Development Core Team (2009). *R: A Language and Environment for Statistical Computing*. Vienna: R Foundation for Statistical Computing: http://www.R-project.org.
Rayner, J. M. V. (1979). A vortex theory of animal flight. Part 2. The forward flight of birds. *J. Fluid Mech.* **91**, 731-763.
Ribak, G., Weihs, D. and Arad, Z. (2005). Submerged swimming of the great cormorant *Phalacrocorax carbo* sinensis is a variant of the burst-and-glide gait. *J. Exp. Biol.* **208**, 3835-3849.
Rosén, M. and Hedenström, A. (2001). Testing predictions from flight mechanical theory: a case study of Cory's shearwater and Audouin's gull. *Acta Ethol.* **3**, 135-140.
Sakamoto, K. Q., Sato, K., Ishizuka, M., Watanuki, Y., Takahashi, A., Daunt, F. and Wanless, S. (2009). Can ethograms be automatically generated using body acceleration data from free-ranging birds? *PLoS ONE* **4**, e5379.
Sato, K., Mitani, Y., Cameron, M. F., Siniff, D. B. and Naito, Y. (2003). Factors affecting stroking patterns and body angle in diving Weddell seals under natural conditions. *J. Exp. Biol.* **206**, 1461-1470.
Sato, K., Daunt, F., Watanuki, Y., Takahashi, A. and Wanless, S. (2008). A new method to quantify prey acquisition in diving seabirds using wing stroke frequency. *J. Exp. Biol.* **211**, 58-65.
Sato, K., Sakamoto, K. Q., Watanuki, Y., Takahashi, A., Katsumata, N., Bost, C.-A. and Weimerskirch, H. (2009). Scaling of soaring seabirds and implications for flight abilities of giant pterosaurs. *PLoS ONE* **4**, e5400.
Schmidt-Nielsen, K. (1972). Locomotion: energy cost of swimming, flying, and running. *Science* **177**, 222-228.
Shamoun-Baranes, J., van Loon, E., Liechti, F. and Bouten, W. (2007). Analyzing the effect of wind on flight: pitfalls and solutions. *J. Exp. Biol.* **210**, 82-90.
Spear, L. B. and Ainley, D. G. (1997). Flight speed of seabirds in relation to wind speed and direction. *Ibis* **139**, 234-251.
Videler, J. J. (2005). *Avian Flight*. New York: Oxford University Press.
Wakeling, J. M. and Hodgson, J. (1992). Optimisation of the flight speed of the little common and sandwich tern. *J. Exp. Biol.* **169**, 261-266.
Watanabe, Y. Y., Takahashi, A., Sato, K., Viviant, M. and Bost, C.-A. (2011). Poor flight performance in deep-diving cormorants. *J. Exp. Biol.* **214**, 412-421.
Weimerskirch, H., Bonadonna, F., Bailleul, F., Mabille, G., Dell'Omo, G. and Lipp, H.-P. (2002). GPS tracking of foraging albatrosses. *Science* **295**, 1259.
Welham, C. V. J. (1992). Flight speeds of migrating birds: a test of maximum range speed predictions from three aerodynamic equations. *Behav. Ecol.* **5**, 1-8.
Yoda, K., Tajima, T., Sasaki, S., Sato, K. and Niizuma, Y. (2012). Influence of local wind conditions on the flight speed of the great cormorant *Phalacrocorax carbo*. *Int. J. Zool.* **2012**, 1-7.
Young, I. R., Zieger, S. and Babanin, A. V. (2011). Global trends in wind speed and wave height. *Science* **332**, 451-455.
Zar, J. H. (2010). *Biostatistical Analysis*, 5th edn. New Jersey: Prentice Hall.